Estimation of vibration limit cycles from wheel/rail mobilities for the prediction of curve squeal noise

Olivier Chiello, Rita Tufano, Martin Rissmann

Estimation of vibration limit cycles from wheel/rail mobilities for the prediction of curve squeal noise

Olivier Chiello[1], Rita Tufano[2] and Martin Rissmann[2]

[1] UMRAE, Univ Gustave Eiffel, IFSTTAR, CEREMA, Univ Lyon, F-69675, Lyon, France
olivier.chiello@univ-eiffel.fr

[2] Vibratec, Railway Business Unit, 28 chemin du petit bois, 69131 Ecully Cedex, France

Abstract. A novel method for the approximate estimation of curve squeal sound levels is proposed. The method directly targets the stationary regime by using wheel/rail mobilities at contact instead of modal characteristics of the structures. The condensation allows a more general description of the dynamics of the structures, in particular the behavior of the rail for which a modal representation is not very suitable. The method is first validated in the case of a reduced modal description of the system by comparing results to a reference cycle obtained by numerical integration in the time domain. It is then applied to realistic cases for which the wheel/rail mobilities are obtained from more elaborated models. The model can be used to carry out parametric studies allowing to design squeal noise mitigation solutions.

Keywords: Curve squeal, Instability, Self-sustained vibrations, Power balance.

1 Introduction

Since Rudd [1], most of the works in the literature agree to attribute the generation of wheel/rail squeal noise in curves to the high lateral slip imposed in the curve and to the resulting instabilities [2]. In squeal models, the occurrence of the phenomenon is thus generally studied through a stability analysis based on the linearization of the contact forces. Two families of methods are used: those leading to a generalized eigenvalue system via a modal description of the system [3] and those describing the wheel/rail interaction at the contact's degrees of freedom using their respective mobilities (Nyquist criterion) [4].

Despite its undeniable interest, stability analysis does not allow the prediction of the amplitudes of the nonlinear self-sustained vibrations resulting from instabilities. These nonlinear vibrations are most often calculated using a numerical integration of the dynamic equations of the system in the time domain, by using either a modal description [3] or a contact condensation from the wheel/rail impulse responses [5]. The possible stationary regimes or "limit cycles" obtained are then re-expressed in the frequency domain. A disadvantage is that the integration has to be carried out over a sufficiently long period of time for the transient regime to stabilize.

Some authors have proposed simplified methods allowing a direct computation of stationary regimes [1,6,7]. These methods are mainly based on the assumption of mono-harmonic limit cycles. Unfortunately, they are limited to a reduced modal description of the system dynamics. In this paper, a more general method using wheel/rail mobilities is proposed to determine approximate limit cycles.

2 Proposed approach

The pass-by of a guided vehicle at speed V in a curve of small radius is considered. The key parameter is the angle of attack α which designates the misalignment of the wheel axis with the rolling direction tangent to the rail. The resulting lateral slip of the wheel on the rail head is given by $V_t \approx \alpha V$. The interaction of a single wheel with the rail is considered and the flange contact is disregarded. The wheel/rail interaction is point-like and reduced to two degrees of freedom, normal and tangential. The wheel and the rail are described by their point and cross contact mobilities Y_{Wtt}, Y_{Wnn}, Y_{wtn}, Y_{Rtt}, Y_{Rnn} and Y_{Rtn} in the frequency domain where subscripts W, R, n and t stand for wheel, rail, normal and tangential degree of freedom. These mobilities can be determined using various types of models.

2.1 Contact and friction laws

The contact is modelled by Hertz's normal stiffness k_H and Mindlin's tangential stiffness ξk_H leading to normal and tangential point mobilities $Y_{Cnn} = j\omega k_H^{-1}$ and $Y_{Ctt} = j\omega\xi k_H^{-1}$ (see for instance rolling noise models [8]) while a non-linear friction/creep law is considered relating the total friction force f_t acting at the wheel/rail interface to the wheel/rail creep s and the normal contact force f_n:

$$f_t(s, f_n) = \mu(s, f_n) f_n \quad \text{with} \quad s = (V_t + \Delta v_t)/V \tag{1}$$

where μ denotes the non-linear dynamic friction coefficient and $\Delta v_t = v_{Wt} - v_{Rt} - v_{Ct}$ stands for the relative instantaneous tangential velocity at the wheel/rail interface. In this paper, the choice was made for a non-linear creep law of Shen-Hedrick-Elkins type [2,4], combined with a heuristic velocity-weakening friction coefficient, but this choice does not restrict the generality of Eq. (1).

2.2 Stability analysis

A stability analysis is first performed using the Nyquist criterion as proposed by De Beer *et al* [4]. For small oscillations around the quasi-static equilibrium characterized by normal load N, lateral creep $s \approx \alpha$ and quasi-static friction force $T = \mu(\alpha, N)N$, the dynamic part of the friction force can be linearized. Considering furthermore harmonic variations of the oscillations such that $\Delta v_t = \Delta\hat{v}_t e^{i\omega t}$, $f_t - T = \hat{f}_t e^{i\omega t}$ and $f_n - N = \hat{f}_n e^{i\omega t}$, the wheel, rail and contact mobilities can be used to express the normal and tangential coupling between the components in the frequency domain:

$$Y_{nn}\widehat{f_n} + Y_{nt}\widehat{f_t} = 0 \quad \text{and} \quad Y_{tn}\widehat{f_n} + Y_{tt}\widehat{f_t} = \Delta\widehat{v_t} \tag{2}$$

where $Y_{nn} = Y_{Wnn} + Y_{Rnn} + Y_{Cnn}$, $Y_{tt} = Y_{Wtt} + Y_{Rtt} + Y_{Ctt}$ and $Y_{nt} = Y_{tn} = Y_{Wnt} + Y_{Rnt}$ are the total contact mobilities. A complex equation $\widehat{f_t} = H(\omega)\widehat{f_t}$ is obtained for the friction force, where closed-loop transfer function $H(\omega)$ is given in [4] as a function of total contact mobilities. According to the Nyquist criterion, oscillations are unstable for pulsations ω such that $\Im(H(\omega)) = 0$ and $\Re(H(\omega)) > 1$. This technique is useful to find the pulsations where instabilities may occur and initiate self-sustained vibrations but does not give any information on the amplitude of these vibrations.

2.3 Power balance for non-linear harmonic cycles

Considering larger oscillations around the quasi-static equilibrium, the friction force can no longer be linearized and in most cases the frequency domain is not appropriate to describe the response of the structure. Nevertheless, a mono-harmonic response of the structure is assumed at pulsation ω_i for which the system is unstable, such that $\Delta v_t(t) = \Re(\Delta\widehat{v_t}e^{i\omega_i t})$. With this assumption the power dissipated in the system can be evaluated analytically with linear harmonic techniques (i.e. from Eqs. (2)) since the behavior in the structure remains linear:

$$\overline{W_{\text{dis}}} = \frac{1}{2}\,\Re(\Delta\widehat{v_t}f_t^*) = \frac{|\Delta\widehat{v_t}|^2}{2}\,\Re((Y_{tt} - Y_{tn}Y_{nn}^{-1}Y_{nt})^{-1}) \tag{3}$$

However, for the evaluation of the injected power a time integration over the cycle has to be performed since the friction force is non-linear:

$$\overline{W_{\text{inj}}} = \frac{1}{T}\int_0^T \Delta v_t(t)\mu\big(s(t), f_n(t)\big)f_n(t)dt \tag{4}$$

where $s(t) = \alpha + \frac{1}{V}\Re(\Delta\widehat{v_t}e^{i\omega_i t})$ and $f_n(t) = N + \Re((Y_{tn} - Y_{tt}Y_{nt}^{-1}Y_{nn})^{-1}\Delta\widehat{v_t}e^{i\omega_i t})$ is directly expressed as a function of $\Delta v_t(t)$ from Eqs. (2).

The ntegral (4) may be computed numerically for a given value of amplitude $\Delta\widehat{v_t}$. It is important to note that, unlike dissipated power $\overline{W_{\text{dis}}}$, injected power $\overline{W_{\text{inj}}}$ is not proportional to $|\Delta\widehat{v_t}|^2$ so that the power balance may vary with $\Delta\widehat{v_t}$ and differ from the linear case (see ref. [9] in this case). The search for stationary self-sustained vibrations thus amounts to find $\Delta\widehat{v_t}$ such that:

$$\overline{W_{\text{inj}}}(\Delta\widehat{v_t}) = \overline{W_{\text{dis}}}(\Delta\widehat{v_t}) \tag{5}$$

which consists in solving a nonlinear algebraic equation on $\Delta\widehat{v_t}$.

2.4 From the amplitude of the cycle to the radiated sound power

In cases where a solution is found to Equation (5), complex magnitudes $\widehat{f_t}$ and $\widehat{f_n}$ of the tangent and normal forces acting at the wheel/rail interface at unstable pulsation ω_i are calculated using Eqs. (2). The sound power radiated by the wheel is finally estimated from contact forces by a “rolling noise” type method based on analytical radiation factors [8].

3 Validation for a reduced wheel/rail model

The method was tested on the reduced model proposed in [10] and shown in Fig. 1. The wheel and rail are each modelled by a mass-spring-damper system tuned to a particular mode. Angle θ is related to the ratio of the normal and tangential contributions of the wheel mode. For the rail, only the normal dynamics are considered. For the wheel, parameters have been adjusted to the axial mode $0L4$ of the wheel modelled in Sec. 4. For the rail, the reduction to one mode is not very realistic: the parameters were simply chosen to obtain the same normal mobility (modulus and phase) as the model used in Sec. 4 at the natural frequency of the wheel mode (1850 Hz).

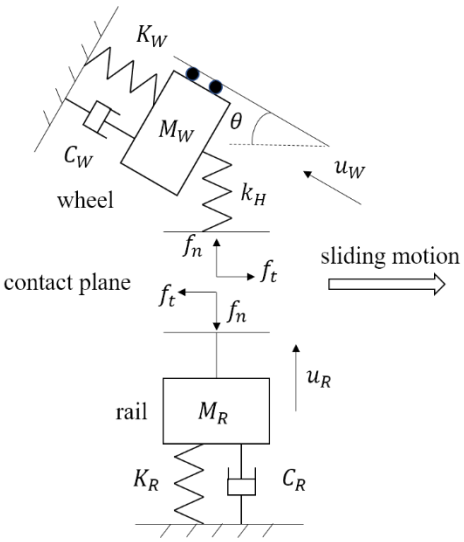

Fig. 1. Schematic of the reduced model used for the validation of the method

3.1 Expression of contact mobilities and stability analysis

For such a system, the contact mobilities are simply written:

$$\begin{gathered} Y_{nn} = Y_W \sin\theta^2 + Y_R + j\omega k_H^{-1} \\ Y_{tt} = Y_W \cos\theta^2 \\ Y_{nt} = Y_W \sin\theta \cos\theta \\ \text{with } Y_W = j\omega(-M_W\omega^2 + j\omega MC_W + K_W) \\ \text{and } Y_R = j\omega(-M_R\omega^2 + j\omega MC_R + K_R) \end{gathered} \tag{6}$$

Closed-loop transfer function $H(\omega)$ can be easily computed from these mobilities, and linearized form of creep/friction law $f_t(s, f_n)$ as described in [4,9]. With the tuned parameters, the Nyquist criterion shows that the system is unstable at a frequency close to the natural frequency of the wheel mode.

3.2 Numerical integration in the time-domain

In order to obtain a reference solution, a numerical integration of the nonlinear equations corresponding to the reduced model (see [7] for instance) has been performed in the time domain. A small initial tangential velocity of 10^{-3} m/s has been used to accelerate the development of the self-sustained vibrations from the quasi-static equilibrium. The evolution of the tangential velocity over the whole integration time (1 s) is given on the left of Fig. 2. On the right, only the five last milliseconds are plotted. A transient increase due to instability is observed, followed by the establishment of a quasi-harmonic periodic stationary oscillation at a fundamental frequency of 1847 Hz and an amplitude of 0.0585 m/s.

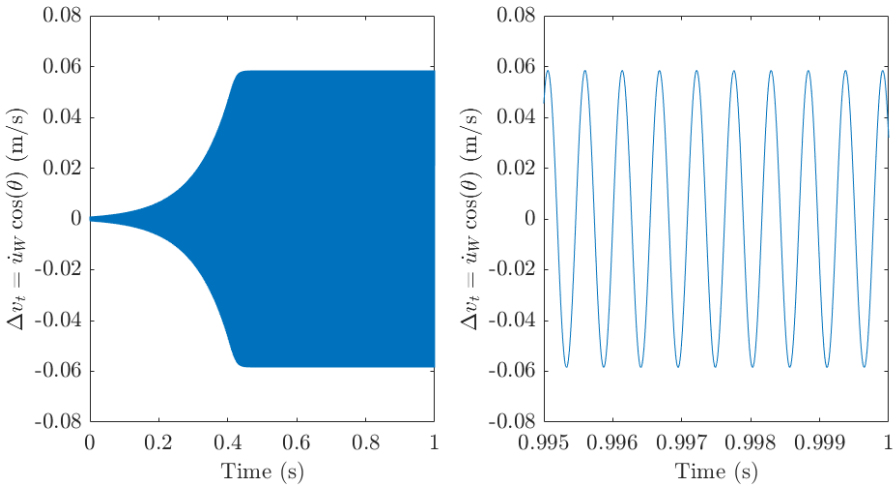

Fig. 2. Solution obtained by numerical integration in the time-domain

3.3 Results obtained with the proposed approach

Non-linear Equation (5) is then solved at the frequency where instability occurs, from contact mobilities given in Eq. (6) and non-linear form of creep/friction law $f_t(s, f_n)$, leading to a solution $\Delta\widehat{v_t} = 0.0585$ m/s. This result is remarkably good as it corresponds to an error of less than 0.02% compared to the reference value obtained with the numerical integration.

Details of the variations of the injected and dissipated powers (normalized by $|\Delta\widehat{v_t}|^2$) are plotted on Fig. 3 as a function of $\Delta\widehat{v_t}$. The figure highlights the difference between the linear domain (amplitudes $\Delta\widehat{v_t} < 0.05$ m/s) where the normalized powers are both constant and the non-linear domain (higher amplitudes $\Delta\widehat{v_t} > 0.05$ m/s) where the normalized injected power decreases with the amplitude of the cycle until it reaches the normalized dissipated power at the solution value.

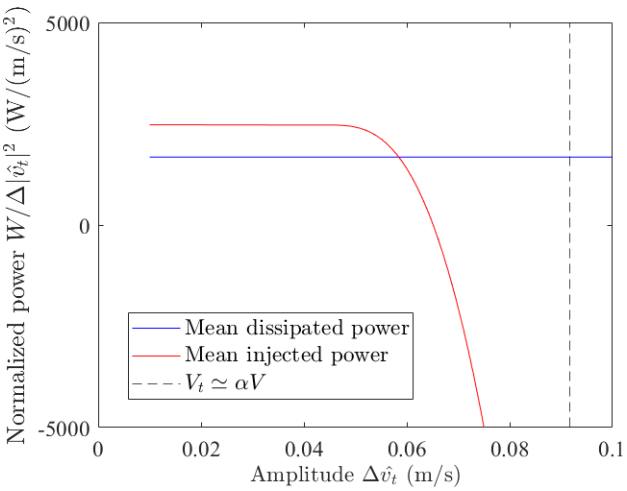

Fig. 3. Power balance as a function of the cycle amplitude for the reduced model

4 Results obtained with more elaborated models

4.1 Components models and input data

The method is tested in a realistic case of a metro wheel rolling in a curve at speed $V = 30$ km/h and angle of attack $\alpha = 11$ mrad. At this angle of attack and for the chosen friction parameters, the friction/creep curve is decreasing which reflects a potential source of instability. A normal load $N = 51$ kN is considered. The wheel is a steel monobloc wheel with a diameter of 86 cm. It is first modelled by the Finite Element Method considering clamped boundary conditions at the axle axis. Contact mobilities are computed by modal superposition from 37 normal modes obtained with the Finite Element model in the frequency range 0 – 6250 Hz. Damping factors of 0.01 % are chosen for most of modes above 400 Hz. A classical "Rodel" model (infinite Timoshenko beam with uniform elastic support [8]) is chosen for the rail lying on monobloc concrete sleepers through elastic rail pads of medium stiffness. Contact mobilities are computed analytically from rail and support parameters.

The stability analysis performed by using the Nyquist criterion highlights 9 frequencies where instabilities may occur. They correspond for the most part to the natural frequencies of axial wheel modes without nodal circles. These modes are known to play an important role in the generation of curve squeal.

4.2 Non-linear harmonic cycles and radiated sound power

Non-linear Equation (5) is solved for each frequency where instability may occur. For each of them an amplitude $\Delta\widehat{v_t}$ is found, leading to a balance between the injected and dissipated powers. The corresponding radiated sound powers are given in Fig. 4. It can

be observed that the amplitudes are quite similar for all modes. Even though this simple model cannot predict which mode(s) or set of modes will actually be present in the solution, computed sound powers provide a first estimation of the squeal noise potentially emitted by the system for one given unstable mode. The levels obtained for the $0L0$ and $0L1$ modes are however questionable, as these modes are generally not found in field measurements. The single wheel model used here is probably not sufficient to fully understand the dynamics of these low-frequency modes, due to the potential influence of bending axle modes on the wheel mobility.

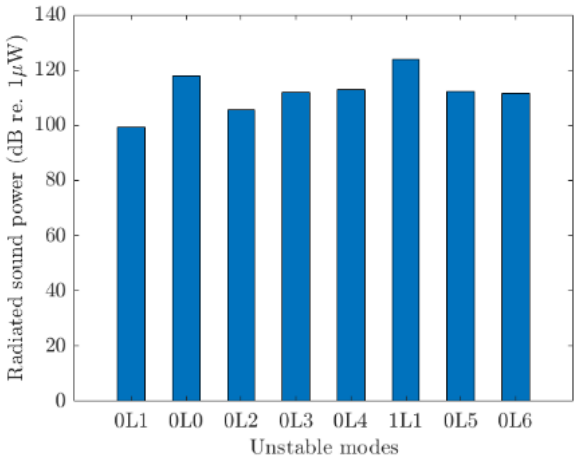

Fig. 4. Radiated sound power for each unstable mode

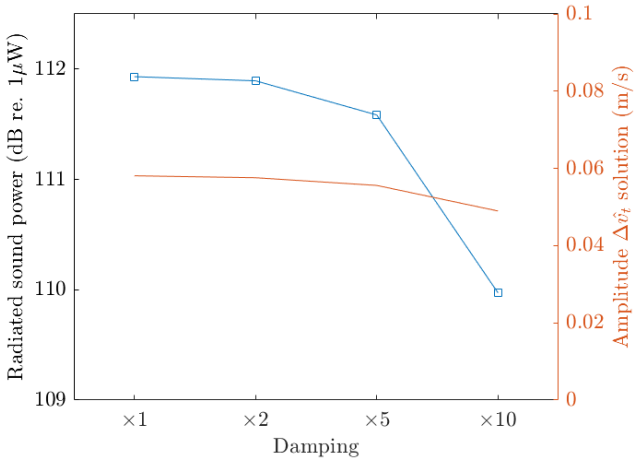

Fig. 5. Influence of damping on radiated sound power (mode $0L4$)

4.3 Effect of wheel damping

The effect of wheel damping is studied to illustrate possible parametric studies with the simplified approach. Fig. 5 shows the results obtained for the mode $0L4$ with damping factors of 0.02 %, 0.05 % and 0.1 % compared with a nominal damping factor of 0.01%. It is important to note that a critical damping factor of 0.11 % is sufficient to stabilize the mode. It can be observed that the amplitude of the cycle as well as the radiated power are very little sensitive to the damping factor except near the critical damping, which reflects a strongly non-linear behavior.

5 Conclusion

A novel method for the approximate estimation of curve squeal levels is proposed, directly targeting the non-linear stationary regime and using wheel/rail mobilities at contact instead of modal characteristics of the structures. As for the stability analysis or the time integration, the condensation at contact allows a more general and more functional description of the dynamics of the structures, in particular the behaviour of the rail for which a modal representation is not very suited. The method is applied to a realistic case for which the wheel and rail mobilities are obtained from elaborated models. It proves to be very efficient and adapted to parametric studies aiming to design curve squeal noise mitigation solutions.

References

1. Rudd M. J. Wheel/rail noise—Part II: Wheel squeal. *Journal of Sound and Vibration*, **46**, 381—94 (1976).
2. Thompson D. J., Squicciarini G., Ding B. and Baeza L. A State-of-the-Art Review of Curve Squeal Noise: Phenomena, Mechanisms, Modelling and Mitigation. In: Anderson D. *et al.* (eds) Noise and Vibration Mitigation for Rail Transportation Systems. *Notes on Numerical Fluid Mechanics and Multidisciplinary Design*, **139**, 3—41 (2018). Springer, Cham.
3. Chiello O., Ayasse J.-B., Vincent N. and Koch J.-R. Curve squeal of urban rolling stock—Part 3: Theoretical model. *Journal of Sound and Vibration*, **293**, 710—27 (2006).
4. De Beer F. G., Janssens M. H. A. and Kooijman P. P. Squeal noise of rail-bound vehicles influenced by lateral contact position. *Journal of Sound and Vibration*, **67**, 497—507 (2003).
5. Pieringer A. A numerical investigation of curve squeal in the case of constant wheel/rail friction. *Journal of Sound and Vibration*, **333**, 4295—4313 (2014).
6. Meehan P. A. and Liu X. Modelling and mitigation of wheel squeal noise amplitude. *Journal of Sound and Vibration*, **413**, 144—58 (2018).
7. Meehan P. A. Prediction of wheel squeal noise under mode coupling. *Journal of Sound and Vibration*, **465**, 115025 (2020).
8. Thompson D. J. Railway Noise and Vibration: Mechanisms, Modelling and Means of Control. Elsevier (2009).
9. Chiello O, Tufano R. and Rissmann M. Modelling of wheel/rail squeal noise in curves from mono-harmonic vibratory limit cycles. In: *InterNoise 2022*, Glasgow, UK (2022).
10. Ding B., Squicciarini, G., Thompson D. J. A. Effect of rail dynamics on curve squeal under constant friction conditions. *Journal of Sound and Vibration*, **442**, 183-199 (2019).